Variable stars in the field of open cluster NGC 6819 – II

R. A. Street,[1]* Keith Horne,[2] T. A. Lister,[2] A. Penny,[3] Y. Tsapras,[4] A. Quirrenbach,[5] N. Safizadeh,[6] J. Cooke,[7] D. Mitchell[7] and A. Collier Cameron[2]

[1]*APS Division, Department of Pure and Applied Physics, Queen's University Belfast, University Road, Belfast BT7 1NN*
[2]*School of Physics and Astronomy, University of St Andrews, North Haugh, St Andrews, Fife KY16 9SS*
[3]*Rutherford Appleton Laboratories, Chilton, Didcot, Oxfordshire OX11 0QX*
[4]*Queen Mary University, School of Mathematical Sciences, Mile End Road, London E1 4NS*
[5]*Sterrewacht Leiden, Universiteit Leiden, PO Box 9513, 2300 RA, Leiden, the Netherlands*
[6]*California Institute of Technology, M/C 100-22, Pasadena, CA 91125, USA*
[7]*Center for Astrophysics and Space Sciences, University of California, San Diego, 9500 Gilman Drive, La Jolla, CA 92093-0424, USA*

ABSTRACT

We report on the discovery of 141 further variable stars found in the field of the open cluster NGC 6819. The stars were identified from time-series photometric data obtained on the Isaac Newton Telescope, La Palma, during two observing runs covering the 19 nights between 1999 June 22–30 and 1999 July 22–31. The variables found include 53 eclipsing binaries, of which eight stars appear to be RS CVns, in addition to 70 stars showing spot activity, 13 showing long-period variability and five variables of other types.

Key words: binaries: eclipsing – stars: variables: other – open clusters and associations: individual: NGC 6819.

1 INTRODUCTION

We observed the intermediate-age open cluster NGC 6819 as part of a search for transits by extrasolar planets. The field was observed with the Wide Field Camera (WFC) on the Isaac Newton Telescope (INT), La Palma over 19 nights in 1999 June and July. We monitored the magnitudes of over 38 000 stars in every exposure. The reduction procedure, developed by studying the central CCD (4) data, automatically identifies photometric variable stars; these were presented in Street et al. (2002) (Paper I). We now present the variable stars discovered in the three remaining WFC CCDs.

Street et al. (2002) tabularized the basic parameters (Table 1) of the open cluster NGC 6819 and presented a summary of the previous studies made. While some variable stars were identified in these works, they are all bright enough to be saturated in our data and we cannot provide further information on them. The radius of this cluster (∼9.5 arcmin; Kalirai et al. 2001) indicates that the vast majority of its stars lie on CCD 4, and so the variables presented here are drawn from the field star population and are not likely to be cluster members.

In Sections 2 and 3 we describe the observations made and the data reduction pipeline developed during the reduction of this first subset of the data. In Section 4 we present the photometry of the variables, with coordinates supplied for follow-up work, while we summarize the work in Section 5.

2 OBSERVATIONS

We observed NGC 6819 for the 19 nights between 1999 June 22–30 and 1999 July 22–31, on the 2.5-m INT, La Palma, using the WFC. This instrument consists of four 2048 × 4096 pixel EEV CCDs, covering a 0.28 deg² field of view with a pixel scale of 0.33 arcsec pix⁻¹. The gain and readout noise were taken from the Cambridge Astronomical Survey Unit (CASU) webpage (http://www.ast.cam.ac.uk/∼wfcsur/ccd.html) and are tabulated in Table 1.

The observations were made using the Sloan r' filter, taking pairs of 300-s exposures. The sequence of exposures was not dithered between frames; we aimed to place each star on the same pixel in each image as far as possible in order to minimize brightness variations due to pixel sensitivies or stars falling between pixels. In practice, the x, y shifts between images were up to a few pixels. NGC 6819 was observed for ∼7–8 h each night, resulting in 16–25 frames per night per CCD, and between ∼360–380 frames in total over the whole run. The average gap between pairs of exposures was, at most, roughly an hour and we had good observing conditions on all nights. The exposure times were tailored to optimally expose the fainter cluster stars for the benefit of transit hunting, which is why many of the stars identified in this cluster by previous authors are saturated in these data. For a figure showing the CCD layout relative to the cluster field, please refer to fig. 1 in Street et al. (2003).

3 DATA REDUCTION

3.1 Point spread function fitting photometry

The data reduction pipeline used to process this data set was described in detail in Street et al. (2002). Following the debiasing,

---

* E-mail: r.street@qub.ac.uk

Table 1. The parameters of each of the INT WFC CCDs. These values were taken from the CASU webpage (http://www.ast.cam.ac.uk/~wfcsur/ccd.html).

CCD	Bias level	Gain (e-/ADU)	Readout noise (e-)	Max ADU
1	1559	3.12	7.9	58 000
2	1636	3.19	6.4	59 000
3	1744	2.96	8.3	59 000
4	1190	2.22	8.4	58 000

flat-fielding and trimming of the frames, the preprocessed frames were registered to the nearest pixel and converted into IRAF[1] format.

A reference frame was selected and reduced manually using the IRAF task DAOPHOT (Stetson 1987). DAOFIND identified 9465, 9483 and 9629 stars in CCDs 1–3, respectively. After performing aperture photometry, approximately 100 isolated stars were manually chosen from each reference frame for the derivation of the point spread function (PSF). The process of selecting PSF stars, generating, refining and subtracting the PSF was iterated until a satisfactory PSF was obtained. The same PSF stars were used to generate such a PSF for all subsequent frames, and the PSF was allowed to follow a two-dimensional quadratic spatial function across each frame.

In order to apply suitable values of data-dependent variables for each frame, a script was used to produce an IRAF parameter file for each image. These files were then automatically called during the reduction.

Once the parameter files, the full starlist and the PSF starlist were in place, PSF photometry was performed on the rest of the data set by an automated DAOPHOT script. We chose to have the star positions refitted independently in each frame, having found that the cross-correlation technique aligned the star centroids to around ∼1-pixel accuracy.

The software we developed to handle the self-calibration of the PSF photometry was described in detail in Street et al. (2002). The photometric precision reached is graphically represented in fig. 2 of Street et al. (2003).

Astrometric positions for all the stars in our sample were obtained using the method described in Street et al. (2002). The average rms error in the resulting RA and Dec. are 0.118 and 0.110 arcsec, 0.232 and 0.363 arcsec and 0.289 and 0.294 arcsec for CCDs 1–3, respectively. This corresponds to an rms scatter of less than one pixel on the CCD.

4 RESULTS

In order to identify variable star candidates, we first needed to eliminate from our sample those stars that were poorly measured. Whatever the reason for this, be it saturation, blending, the close presence of a dead column, etc., only stars measured in at least 60 per cent of frames were considered.

The reduced χ^2 of each star relative to the star's mean magnitude was then calculated; these parameters are plotted in Fig. 1. We notice that the main body of points on the reduced χ^2 plot are below the expected value of 1. We believe that this is due to the overestimation of the magnitude errors produced by DAOPHOT, which include default coefficients for the flat-fielding and PSF errors.

A straight line of variable offset and gradient was fitted using the method of least-squares to the 'backbone' of points in this diagram. A good fit was obtained by iteration. The standard deviation of the points around the line ($\sigma_{\chi_\nu^2}$) was computed and in the following iteration, points more than 2σ away from the line were excluded. This process was repeated until the fitted parameters changed by less than 10^{-5} between iterations. Finally, we identified all stars fulfilling the criterion

$$\chi_\nu^2(j) \geqslant \chi_\nu^2[\overline{m(j)}] + \sigma_{\chi_\nu^2}, \tag{1}$$

where $\overline{m(j)}$, and $\chi_\nu^2(j)$ are the mean magnitude and reduced χ^2 of star j, respectively, and $\chi_\nu^2[\overline{m(j)}]$ is the χ^2 predicted for a star of this magnitude by the fitted lines.

The corresponding cut-off line is plotted in Fig. 1. All 1538 stars found above this threshold (CCDs 1–3) were considered candidate variables. The light curves of these stars were then examined to eliminate those showing spurious or residual systematic effects. We believe the main reasons for stars showing unusually high scatter are blending and the presence of CCD flaws, such as dead columns.

This left us with 53, 41 and 47 variable stars from CCDs 1–3, respectively. In some cases we have highlighted suspicions about the photometry due to, for example, severe blending and proximity to the edge of the frame or very bright stars. We provisionally classify these stars below, although these classes should be considered tentative until confirmed by further work. Light curves of the photometry for the stars are also presented in the relevant sections. Visual inspection of the light curves of these stars indicated those that show a high degree of periodicity. A period-finding program was then applied to the data for these stars. This program uses the Lomb method (Press et al. 1992) to obtain a frequency spectrum where the highest peak represents the inverse of the period of variability. A Gaussian was then fitted to the highest peak in each spectrum to accurately determine the peak frequency and hence the period. The periodograms of some stars showed more than one strong frequency, indicating more than one possible period. This was usually because the period was close to the one day alias, or due to very short duration eclipses with few data points, or else because the period of the variation was greater than the length of the data set. In these cases, we have phased the light curves on the most likely period.

Please note that we have used a consecutive numbering system for the stars. We take the CCDs in numerical order, so that the first star detected on CCD 1 is star 1, the first star on CCD 2 is 1 + (number of stars on CCD 1) and so on. This differs from our previous paper (Street et al. 2002), where we only presented stars from one CCD (CCD 4). For clarity, we include the variables found in CCD 4 in the relevant sections/tables, listed with their old ID numbers in brackets.

In the time between reducing the data from CCD 4 and CCDs 1–3 we introduced an improvement in the rejection of cosmic rays from the light curves. We have therefore reapplied our variable selection criteria in a consistent manner to the CCD 4 data. This analysis confirmed the detection of all variables reported in Street et al. (2002), with the exception of star 30 608 (2031), which now falls slightly below the threshold. This star was marked as suspect in this paper owing to its low amplitude and proximity to a CCD flaw. The data for this star have been left out of the analysis in this paper, but remain in Table 12 (see below) for reference.

4.1 Colour data

In Street et al. (2002) we described the procedure used to obtaining an estimate of the V magnitude of each star. This was achieved by cross-identifying stars present in both our data set and that of Kalirai

---
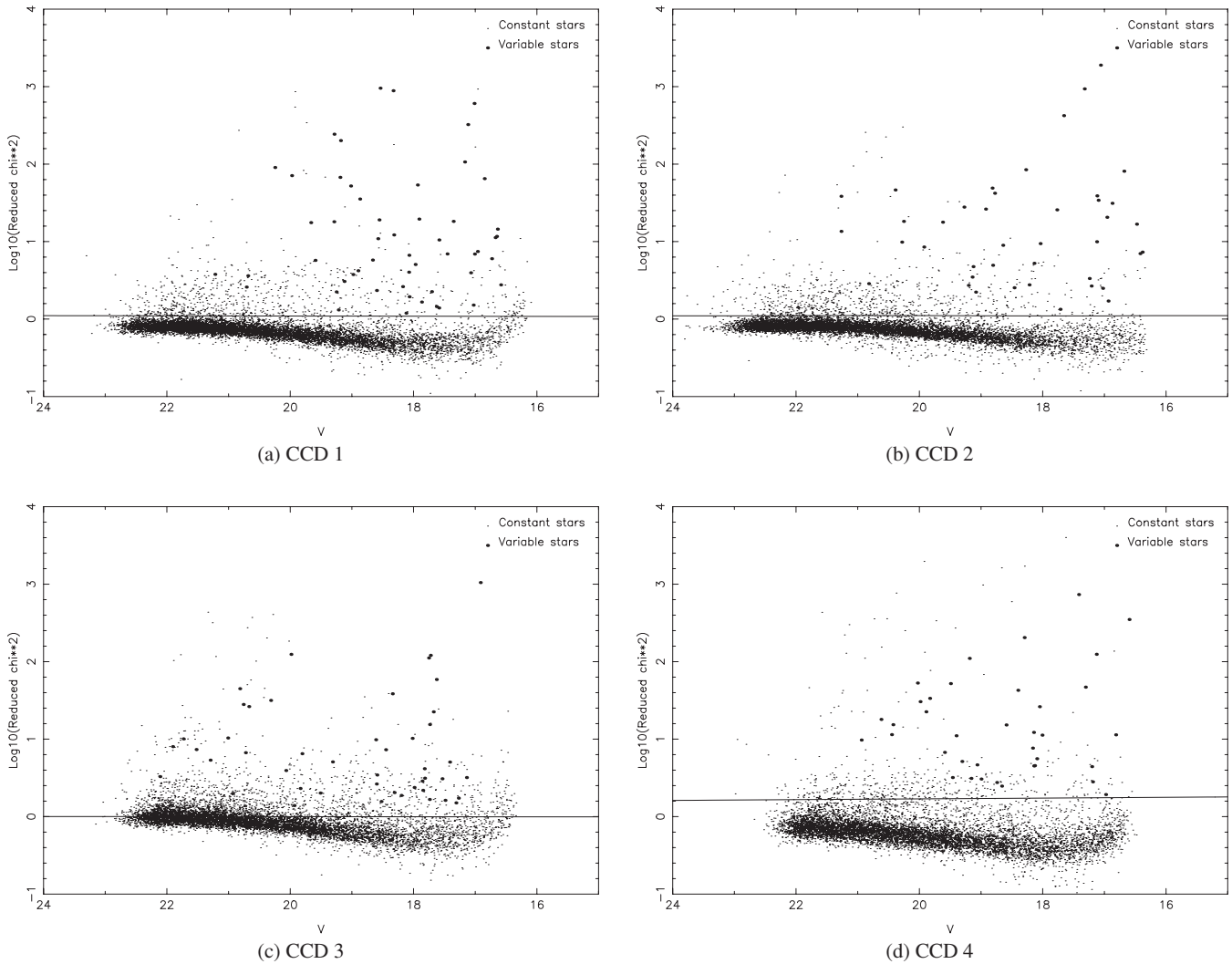
Figure 1. χ^2 fit of a straight line to all light curves plotted against instrumental mean magnitudes.

et al. (2001). The relationships between their calibrated *V* and our instrumental Sloan *r* magnitudes (r_{CCDn}) are given in equation (2) for each WFC CCD. As the overlap between our field and that of Kalirai et al. was not perfect, not all of our stars have *B–V* colours. To obtain (more approximate) estimates of the *V* magnitudes of the remaining stars, we also determined relationships between *r* and *V* without a colour term.

We have derived Sloan *r–i* colour information for these stars from the INT data set. These instrumental colours were related to calibrated *V–R* colours by the same procedure published in Street et al. (2003), but with improved rejection of stars with poor Sloan *i* magnitudes. The calibrations used are given in equation (2). The coefficients determined for each CCD are given in Table 2, and are the same as those presented in Street et al. (2003), with the exception of a small change to the calibration for CCD 1.

$$V = a_0 r_{CCD_n} + a_1$$
$$V = r_{CCD_n} + b_0(B - V) + b_1$$
$$(B - V)_{CCD_n} = (B - V) + c_0$$
$$(r - i)_{CCD_n} = (r - i) + d_0$$
(2)

To summarize the procedure used here, we used the synthetic photometry program XCAL to plot the index *B–V* against *r–i*. This

theoretical model was overlaid on the same instrumental indices plotted for each chip in order to determine the offsets between them (equation 2).

We then used XCAL to plot *V–R* against *r–i* and from these data we determined the relationship:

$$V{-}R = 0.93(r{-}i) + 0.009 \text{ for } -0.2 \leqslant r{-}i \leqslant 0.356$$
$$V{-}R = -1.72\,e^{-1.6.(r{-}i)} + 1.30 \text{ for } 0.356 \leqslant r{-}i \leqslant 2.5.$$
(3)

Fig. 2 presents colour–magnitude diagrams for all CCDs in which the positions of the variables of different types are marked. Only CCD 4 shows an obvious main sequence, because this CCD was centred on the cluster and the radius of the cluster is such that almost all the stars fit within it.

4.2 Eclipsing binaries

We have found 53 eclipsing binary systems, including eight systems which show eclipses and stellar activity. Their details are listed in Tables 3–5. Table 6 lists the eclipsing binaries found in CCD 4. Calibrated *V* magnitudes and *V–R* colour data are listed in columns 6 and 7. However, it should be noted that the colours of the binaries were obtained at unknown phase. This is particularly important for

Table 2. Coefficients for the colour and magnitude calibrations determined for each CCD (see Equation 2).

	$a0$	$a1$	$b0$	$b1$	$c0$	$d0$
CCD1	1.059	−1.66	1.73	1.889	0.2	−0.53
CCD2	1.060	−1.91	0.52	−1.21	0.2	−0.5
CCD3	1.059	−1.74	1.77	2.007	0.2	−0.3
CCD4	1.062	−1.32	0.487	−0.625	0.2	−0.41

some of the larger amplitude binaries. Column 9 of this table lists the peak-to-peak amplitude of the variability.

The phase-folded light curves for these systems are presented in Figs 3–5. Where the variability of the phase-folded light curve is obscured by noise or star activity, we have also shown the unfolded light curve. Most of the eclipsing binaries identified are of the W Ursae Majoris (W UMa; EW) type, while 10 stars seem to be Algol-type (EA) variables. Several stars have noteworthy features which are discussed below.

(i) The period of star 634 appears to be close to 0.5 d. This made it difficult to properly phase the observations. We present the light curve phased on the most likely period, noting the ultrashallow secondary eclipse.

(ii) Stars 1837 and 7823 both show flat-bottomed minima indicative of total eclipses, and of orbits inclined nearly edge-on.

(iii) Star 4539 could be classified as either an Algol-type eclipsing binary or, given the inequality of the maxima, an eclipsing RS Canum Venaticorum (RS CVn) star. Spectroscopic follow-up will be required to distinguish between the two possibilities.

(iv) Several stars show unequal maxima, for example 1920 and 6047. This is probably due to differing star-spot coverage over the face of the stars. The apparent variation in the depth of the secondary eclipse shown by star 4915 is attributed to the same cause.

(v) Star 9257 is an unusual eclipsing binary. The whole light curve is heavily distorted by star-spots. The *V–R* colour indicates a ~G0-type star, while the difference in the depth of the minima suggests a much fainter secondary star. The period is short (0.4218 d), so it seems reasonable that the stars are distorted from spherical. There are several similar cases to be found within the sample; for instance, star 22 520 and perhaps 634.
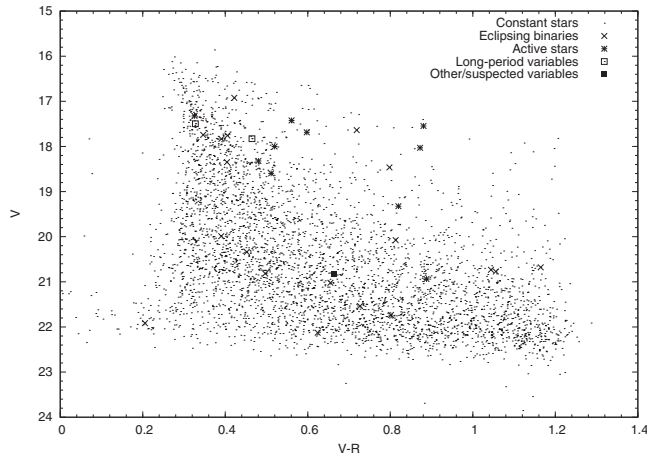
(vi) Eight stars show signs of stellar activity as well as eclipses; these have been classified as RS CVn. We have attempted to provide ephemerides for both periodicities, where possible (listed as 'act' and 'ecl' in Tables 3–5). The fact that few eclipses are observed
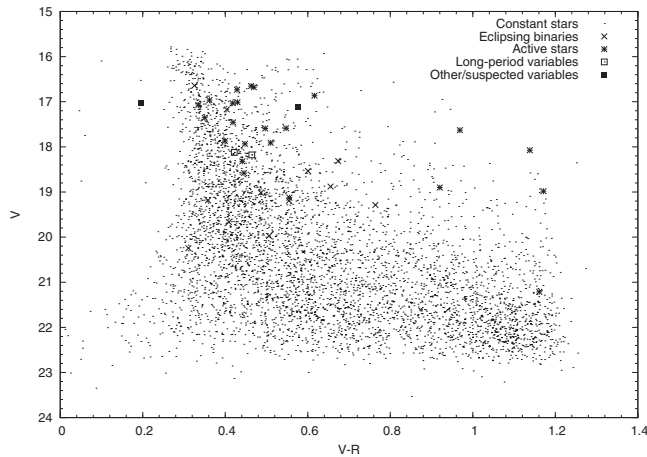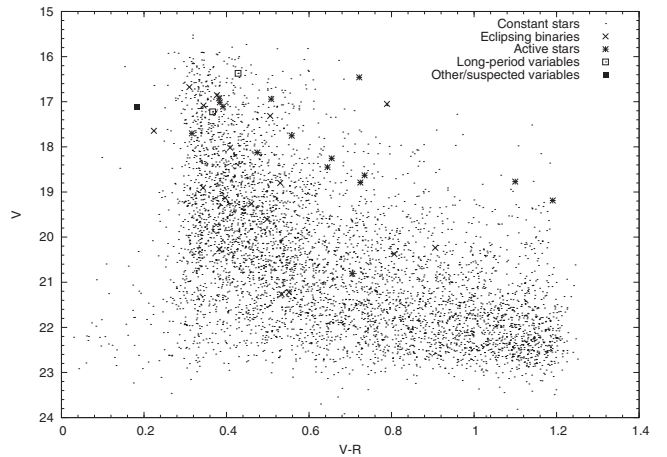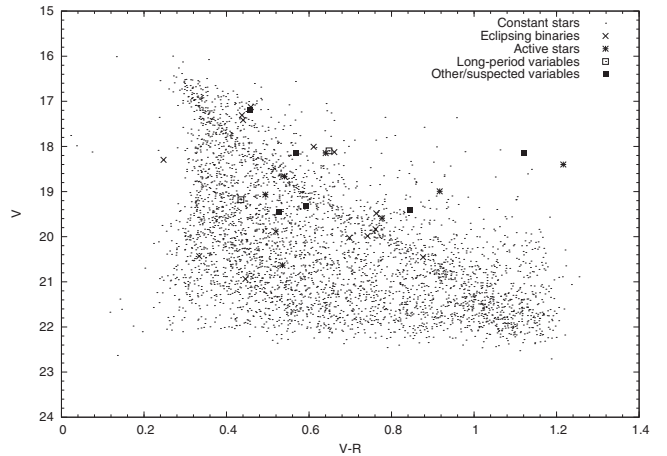

Figure 2. Colour–magnitude diagrams for all four CCDs covering the field of NGC 6819.

Table 3. Details of the eclipsing binary systems from CCD 1, classified into the following categories: W UMa type (EW), Algol type (EA), β Lyrae type (EB) and RS CVn. The error on the last decimal place is given in brackets. Superscripts indicate the following: [C] close bright companions; [B] blended; [E] close to edge of frame; [H] in halo of very bright star.

Star	RA (J2000.0)	Dec. (J2000.0)	Epoch (HJD)	Period (d)	V (mag)	V–R (mag)	Type	Amp. (mag)
249[C]	19 42 15.05	+40 04 42.1	245 1352.535(1)	2.23(3)	18.991(1)	0.7(1)	RS CVn	0.09 (act)
			245 1354.768(1)	4.466(31)				0.2 (ecl)
634[E]	19 42 08.87	+39 53 45.2	245 1358.549(2)	0.4957(7)	19.6(3)		EB?	0.23
1837[B,C]	19 41 54.16	+39 55 28.6	245 1384.566(3)	0.6260(8)	16.6(3)	0.33(9)	EW	0.045
1884	19 41 54.09	+39 59 07.0	245 1358.440(5)	0.27237(14)	18.904(1)	0.6(3)	EW	0.84
1920[C]	19 41 53.93	+40 02 16.6	245 1354.511(5)	0.3639(3)	20.0(4)	0.5(2)	EW	0.4
4539[B]	19 41 21.54	+39 54 36.1	245 1360.426(5)	0.4788(4)	19.3(4)	0.8(2)	EA	0.94
4915[C]	19 41 17.26	+39 56 38.5	245 1354.512(1)	0.3739(2)	17.2(3)	0.40(7)	EW?	0.105
5252	19 41 13.51	+39 57 26.2	245 1356.541(1)	0.2872(887)	19.056(1)	0.6(1)	EW	0.24
6047	19 41 04.28	+40 00 33.2	245 1356.475(7)	0.27213(14)	19.179(2)	0.4(2)	EW	0.38
6690[E]	19 40 56.71	+40 05 05.0	245 1359.03(5)	3.3(5)	18.834(1)		RS CVn	0.02 (act)
			245 1356.5775(7)	10.646(3)				0.1 (ecl)
6781[B]	19 40 55.34	+40 03 35.9	245 1357.489(2)	0.3060(2)	19.558(2)	0.4(1)	EW	0.18
7695	19 40 44.03	+40 03 44.5	245 1386.08(1)	4.6(1)	18.513(1)		RS CVn	0.15 (act)
			245 1383.438(3)	8.5(1)				0.06 (ecl)
7823[C]	19 40 42.01	+39 56 43.6	245 1357.467(2)	0.33995(22)	20.2(4)	0.3(2)	EW	0.47
9040	19 40 24.98	+39 56 08.0	245 1355.570(19)	0.25218(12)	18.3(3)	0.7(2)	EW	0.62
9257	19 40 22.15	+39 55 10.3	245 1354.565(2)	0.4218(14)	19.0(3)	0.5(1)	EW?	0.25

Table 4. Details of the eclipsing binary systems from CCD 2, classified into the following categories: W UMa type (EW), Algol type (EA), β Lyrae type (EB) and RS CVn. The error on the last decimal place is given in brackets. Superscripts indicate the following: [C] close bright companions; [B] blended; [F] close to flaw in image, e.g. dead column, light leak or diffraction spike.

Star	RA (J2000.0)	Dec. (J2000.0)	Epoch (HJD)	Period (d)	V (mag)	V–R (mag)	Type	Amp. (mag)
9789[F]	19 39 24.15	+40 15 46.3	245 1383.495(2)	0.2475(1)	21.2(5)	0.6(3)	EW	0.65
10 400[B]	19 40 05.30	+40 14 17.7	245 1354.586(1)	5.84(2)	18.9(4)	0.34(9)	EA	0.15
10 411[C]	19 39 59.49	+40 14 15.8	245 1356.503(3)	0.2982(2)	19.6(4)	0.50(9)	EB	0.11
10 563[B]	19 39 45.63	+40 13 56.3	–	–	19.3(4)	0.46(9)	EA	0.49
10 748	19 39 54.68	+40 13 30.3	245 1385.602(3)	0.2585(1)	21.3(5)	0.5(2)	EW	0.4
11 620[B]	19 40 03.22	+40 11 25.4	245 1385.565(2)	0.2446(1)	17.0(4)	0.8(3)	EW	0.5
11 625	19 39 29.60	+40 11 23.6	245 1353.523(2)	0.2590(1)	20.4(5)	0.8(2)	EB	0.46
11 644	19 40 13.93	+40 11 21.9	245 1387.8(1)	5.5(16)	19.1(4)	0.40(5)	RS CVn	0.01 (act)
			245 1352.604(4)	4.60(3)				0.05 (ecl)
12 341	19 39 20.19	+40 09 45.3	245 1354.473(4)	0.3828(3)	20.3(5)	0.38(8)	EW	0.11
13 055	19 40 07.59	+40 08 07.2	245 1359.621(4)	0.3903(3)	16.7(4)	0.3(1)	EW	0.09
13 770	19 39 41.89	+40 06 28.8	245 1356.561(2)	0.9097(14)	20.420(3)	0.9(1)	EA	0.41
14 308[C]	19 39 30.42	+40 05 13.4	245 1357.98(8)	5.0(9)	18.755(1)	0.53(8)	RS CVn	0.06 (act)
			245 1383.435(3)	5.4(2)				0.27 (ecl)
14 756	19 39 36.85	+40 04 09.4	245 1356.595(3)	0.5756(6)	17.526(3)	0.2(1)	EB	0.2
14 827[B]	19 39 24.34	+40 03 58.3	245 1359.461(2)	0.3117(2)	17.1(4)	0.34(5)	EW	0.05
16 155[C]	19 40 12.44	+40 00 45.1	245 1389.09(3)	4.0(1)	18.0(4)	0.41(5)	RS CVn	0.01 (act)
			245 1359.528(2)	4.648(10)				0.06 (ecl)
16 763	19 39 43.38	+39 59 15.7	245 1358.482(2)	0.3656(2)	16.915(2)	0.38(5)	EB	0.05
17 589	19 39 20.76	+39 57 22.9	245 1383.739(3)	0.2490(1)	17.3(4)	0.5(2)	EW	0.5

due to the long periods combined with the additional periodicity tends to a confused periodogram, and it was not always possible to distinguish both periods clearly.

Fig. 6 shows the distributions of period and amplitude from the sample of eclipsing binaries (including all types). It is no surprise that the former distribution (Fig. 6a) is dominated (51.5 per cent) by the short-period W UMa-type binaries. The periods of β Lyrae (EB) binaries also cluster at small periods as expected, while those in the EA and RS CVn classes are spread more uniformly. This in-

cludes a population of short-period, undistorted Algol-type binaries, of which several new examples are given. The period and colour information on these systems implies that they consist of late-type stars; such systems are inherently faint and so are lesser known. Fig. 6(c) shows the distribution of the W UMa binaries separately, while Fig. 6(d) plots the distribution of W UMa periods in relationship to their V–R colours. It highlights the presence of one outlier, star 1884, with a period significantly longer than most of our W UMas ($P = 0.6260$ d), but not unusually long for this class of stars ($P \sim 1$ d). Although the colour data used in Fig. 6(d) are V–R and

Table 5. Details of the eclipsing binary systems from CCD 3, classified into the following categories: W UMa type (EW), Algol type (EA), β Lyrae type (EB) and RS CVn. The error on the last decimal place is given in brackets. Superscripts indicate the following: [C] close bright companions; [B] blended; [E] close to edge of frame; [F] close to flaw in image, e.g. dead column, light leak or diffraction spike; [H] in halo of very bright star.

Star	RA (J2000.0)	Dec. (J2000.0)	Epoch (HJD)	Period (d)	*V* (mag)	*V–R* (mag)	Type	Amp. (mag)
20 910[H]	19 41 57.10	+40 18 25.3	245 1383.50(2)	1.31(6)	18.5(3)	0.8(1)	RS CVn	0.02 (act)
			245 1356.470(9)	2.62(1)				0.1 (ecl)
21 744	19 41 46.94	+40 26 59.8	245 1387.469(1)	0.3253(2)	21.0(4)	0.7(2)	EB	0.4
21 816	19 41 45.68	+40 19 23.6	245 1384.203(6)	1.422(3)	17.686(1)	0.35(5)	EB	0.08
22 330	19 41 39.85	+40 23 36.2	245 1382.433(3)	1.37(2)	21.833(8)	0.6(2)	EA	0.7
22 431	19 41 37.91	+40 17 17.3	245 1353.530(1)	0.8908(6)	20.969(5)	1.1(2)	EA	0.7
22 520	19 41 37.21	+40 21 56.2	245 1360.585(2)	0.579(3)	17.875(1)	0.7(1)	EB	0.12
22 695	19 41 34.66	+40 20 36.9	245 1385.572(2)	0.4138(3)	19.511(2)	0.4(3)	EW	0.42
22 790	19 41 33.86	+40 26 35.0	245 1383.454(1)	7.2246(1)	20.1(4)	0.8(1)	EA	0.27
23 228	19 41 28.51	+40 22 59.7	245 1385.790(2)	0.3740(3)	20.518(3)	0.5(2)	EW?	0.65
23 314[H]	19 41 27.66	+40 24 10.6	245 1384.2(2)	0.86(3)	18.281(1)	0.40(5)	RS CVn	0.01 (act)
			245 1383.647(1)					0.58 (ecl)
24 230[H]	19 41 15.77	+40 21 10.2	245 1383.811(9)	0.5504(1)	21.619(7)	0.7(2)	EA	0.9
24 582[C]	19 41 11.23	+40 23 41.1	245 1382.548(5)	10.228(4)	17.754(1)	0.39(5)	EA	0.04
24 837	19 41 08.16	+40 23 00.0	245 1383.536(2)	0.3229(2)	21.600(7)	0.8(2)	EW	0.55
25 493	19 41 00.29	+40 21 27.8	245 1383.495(3)	0.3274(2)	20.890(4)	1.0(1)	EB	0.28
25 645[C]	19 40 57.99	+40 19 00.3	245 1384.486(6)	0.2734(1)	21.588(7)	0.2(2)	EW	0.4
26 668[B]	19 40 44.79	+40 18 05.7	245 1384.655(6)	0.3719(2)	21.3(4)		EW	0.2
27 620	19 40 32.72	+40 22 01.0	245 1357.512(5)	0.3242(2)	17.016(2)	0.4(2)	EW	0.3
27 739[F]	19 40 31.68	+40 26 37.4	245 1354.4922(9)	0.3592(2)	17.8(3)	0.41(9)	EW	0.13
27 861	19 40 29.08	+40 18 02.2	245 1385.763(3)	0.18170(6)	20.898(4)	1.2(2)	EB?	0.4
28 022[C,E]	19 40 27.26	+40 17 21.1	245 1385.639(1)	0.3929(3)	20.141(3)	0.5(2)	EW	0.33
28 559[B,E]	19 40 20.64	+40 27 33.4	245 1359.570(1)	4.678(10)	17.7(3)		EA	0.4

Table 6. Details of the eclipsing binary systems from CCD 4, classified into the following categories: W UMa type (EW), Algol type (EA), β Lyrae type (EB) and RS CVn. The error on the last decimal place is given in brackets. Superscripts indicate the following: [C] close bright companions; [F] close to flaw in image, e.g. dead column, light leak or diffraction spike. The star's original identification number is given in brackets for reference.

Star	RA (J2000.0)	Dec. (J2000.0)	Epoch (HJD)	Period (d)	*V* (mag)	*V–R* (mag)	Type	Amp. (mag)
30 330 (1753)	19 41 52.26	+40 12 23.8	245 1358.6315(4)	0.2751(2)	20.078(3)	0.7(2)	EW	0.43
32 433 (3856)	19 41 28.58	+40 16 24.8	245 1356.4608(34)	0.293(1)	17.246(1)	0.5(1)	EW	0.2
33 018 (4441)[F]	19 41 22.91	+40 14 39.5	245 1358.5536(21)	0.2562(8)	18.275(1)	0.66(9)	EW	0.1
33 025 (4448)[C]	19 41 22.61	+40 11 07.1	245 1359.519(2)	0.3032(2)	17.494(1)	0.44(8)	EW	0.13
33 879 (5302)[C]	19 41 15.27	+40 12 31.8	245 1383.326(4)	0.6742(38)	18.106(1)	0.61(8)	EB?	0.07
34 237 (5660)	19 41 11.73	+40 06 39.7	245 1359.6924(8)	0.3384(2)	18.172(1)	0.2(2)	EW	0.29
34 411 (5834)[F]	19 41 10.33	+40 15 18.3	245 1387.726(1)	0.3660(3)	16.610(2)		EW	0.35
34 807 (6230)	19 41 05.84	+40 12 54.3	245 1382.4676(8)	0.2814(2)	20.724(4)	0.4(1)	EW?	0.27
35 305 (6728)	19 40 59.64	+40 08 25.0	245 1359.516(1)	0.2637(9)	19.811(2)	0.5(1)	EW	0.22
35 910 (7333)	19 40 53.05	+40 11 17.5	245 1385.607(1)	0.3571(2)	20.056(2)	0.8(2)	EA	0.5
36 493 (7916)	19 40 44.83	+40 09 23.0	245 1391.6151(3)	1.468(2)	17.359(3)	0.4(2)	EA	1.2
36 657 (8080)	19 40 42.71	+40 13 25.9	245 1355.5551(5)	0.2899(2)	20.374(3)	0.7(2)	EB	0.3
37 441 (8864)	19 40 31.55	+40 12 51.8	245 1354.569(3)	1.332(3)	20.5(5)	0.3(1)	EA	0.55
37 520 (8943)	19 40 30.48	+40 16 24.1	245 1383.567(1)	0.2705(1)	19.559(2)	0.8(2)	EB	0.35
38 017 (9440)	19 40 21.82	+40 12 08.5	245 1355.628(9)	1.451(4)	20.6(5)	0.9(1)	EB?	0.17

not *B–V*, as used by Rucinski & Duerbeck (1997), our distribution mimics that shown in their fig. 2; hotter stars display longer periods.

4.3 Active stars and long-period systems

We have found 70 stars which appear to be of the BY Dra type; their details are tabulated in Tables 7–9, and their light curves are presented in Figs 7–9. The details of the CCD4 BY Dra-type systems are given in Table 10. In some cases we have noted reason to treat the photometry with caution owing to factors stated in the tables; mostly due to contamination from nearby stars.

While ephemerides have been determined for these stars, in some cases the periods are a sizable fraction of the length of the data set. Therefore, as few complete cycles were observed, the periods show a higher degree of uncertainty. It should also be remembered that the period has been determined from the photometric variations caused by transient star-spots. These can vary in latitude as well as size, where differential rotation can produce a different measured period.

Most of these stars show the classic sinusoidal photometric variations attributed to star-spot activity on time-scales of a few to
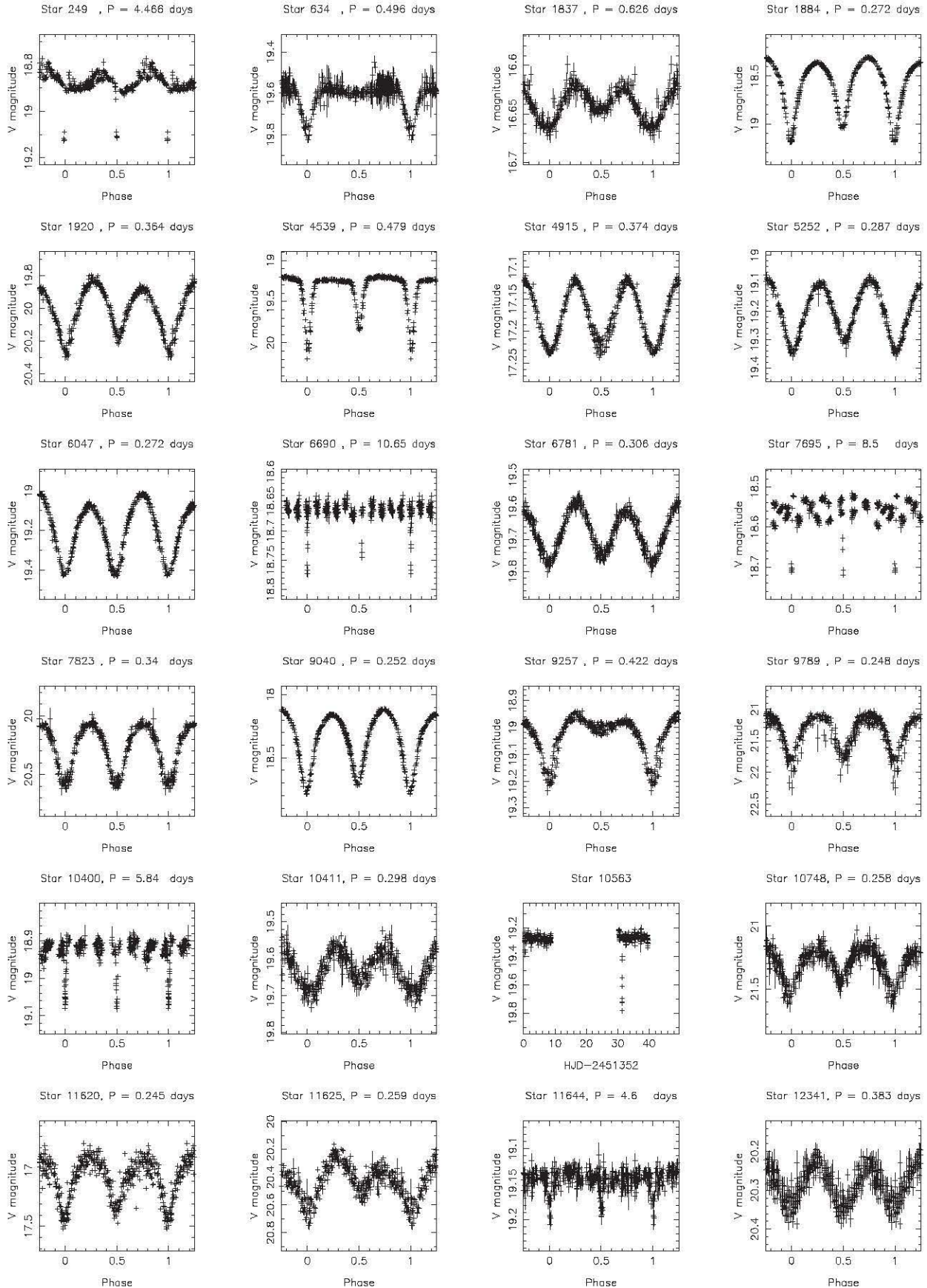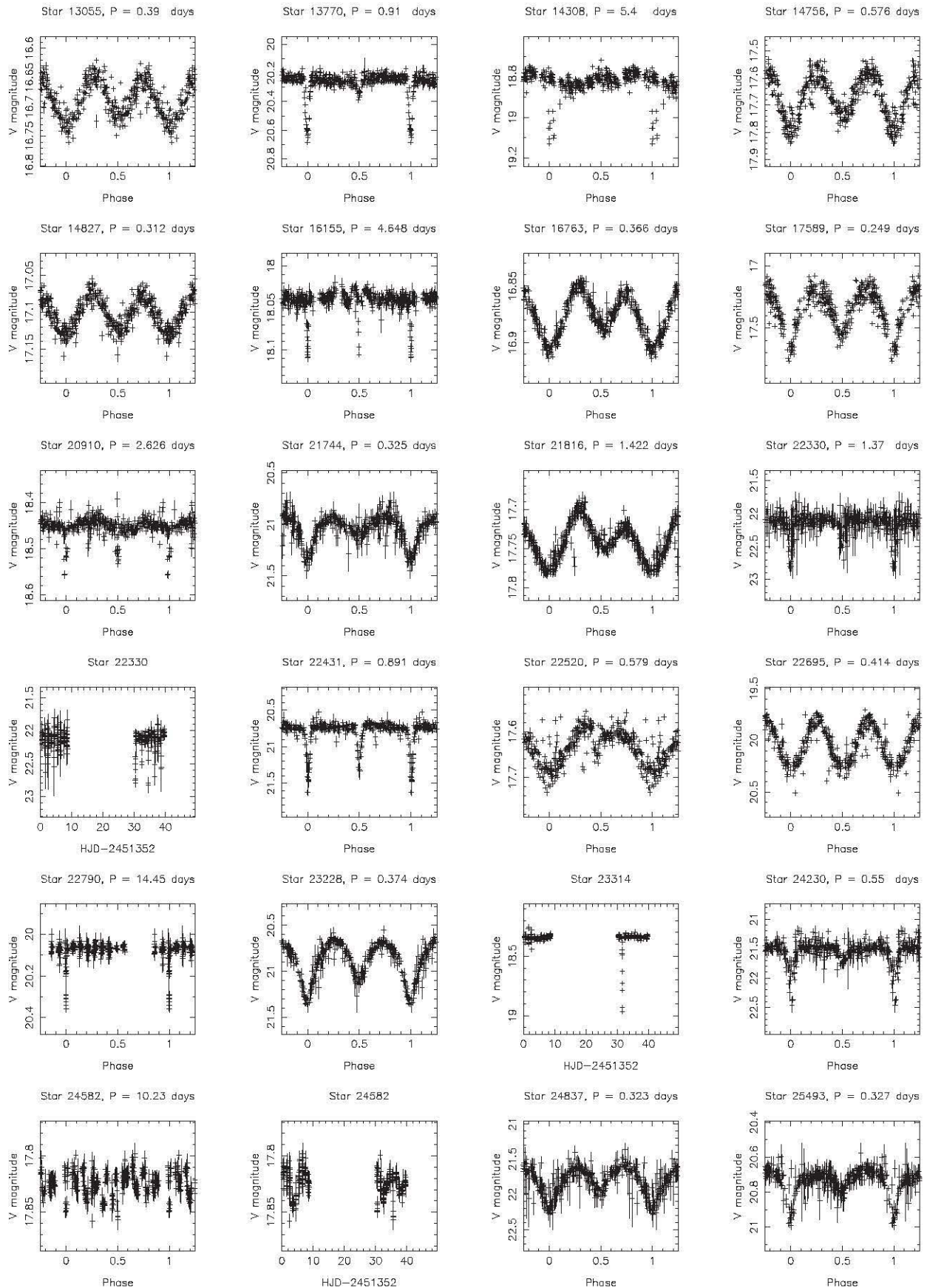
Figure 3. Phased light curves for eclipsing binary systems.

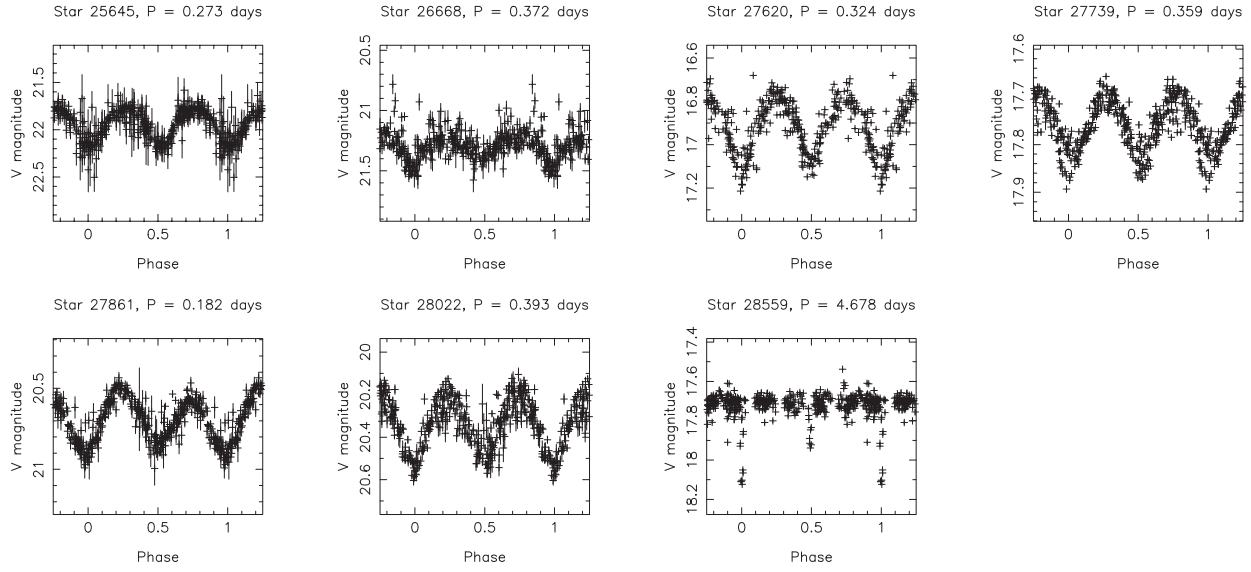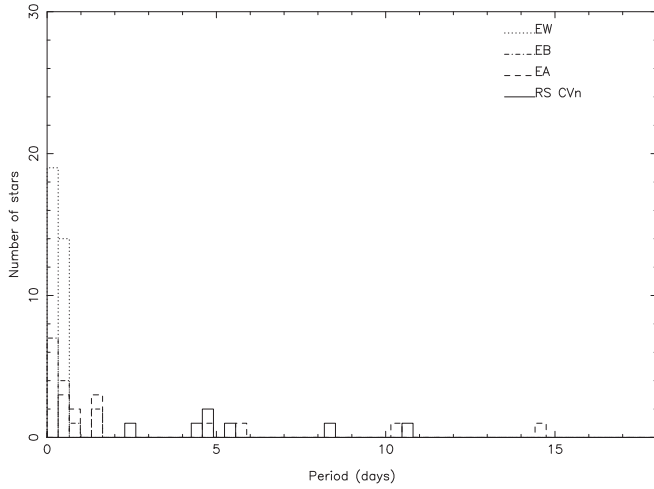**Figure 4.** Phased light curves for eclipsing binary systems.
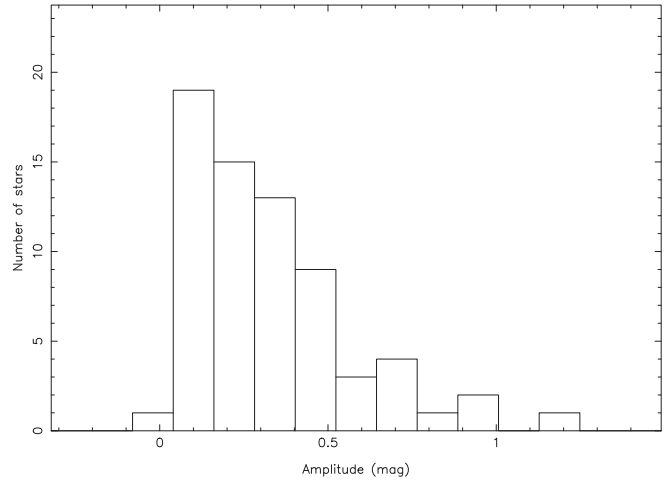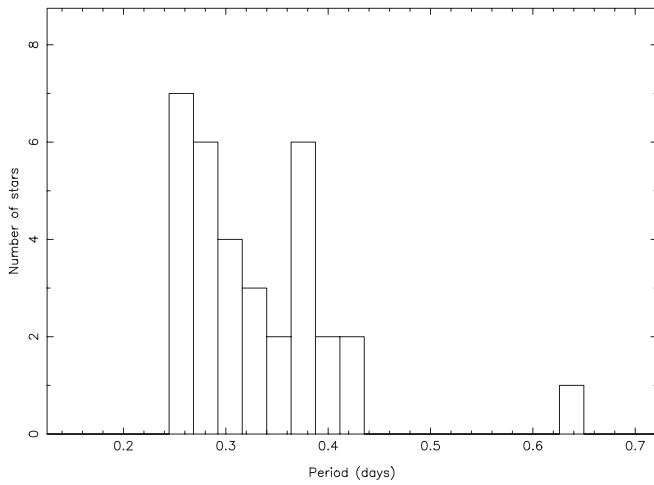
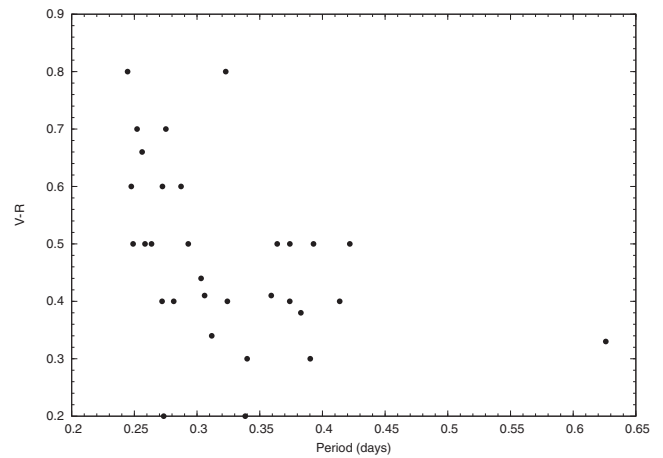**Figure 5.** Phased light curves for eclipsing binary systems.

(a) Distribution of EB periods

(b) Distribution of EB amplitudes

(c) Distribution of W UMa periods

(d) Distribution of W UMa periods and $V - R$ colours

Figure 6. Distributions of the eclipsing binary populations according to period and amplitude.

Table 7. Details of BY Dra-type systems from CCD 1. The error on the last decimal place is given in brackets. Superscripts indicate the following: [C] close bright companions; [B] blended; [E] close to edge of frame; [F] close to flaw in image, e.g. dead column, light leak or diffraction spike; [S] suspected variable.

Star	RA (J2000.0)	Dec. (J2000.0)	Epoch (HJD)	Period (d)	V (mag)	$V–R$ (mag)	Amp. (mag)
33[E]	19 42 17.26	+40 01 45.6	245 1384.991(47)	5.0(2)	18.223(1)		0.03
134[C]	19 42 15.32	+39 55 35.3	245 1354.731(21)	2.44(4)	18.6(3)	0.45(7)	0.07
202[C]	19 42 14.85	+39 56 57.3	245 1385.684(25)	1.455(16)	17.773(1)	0.55(7)	0.06
783	19 42 07.45	+39 58 17.2	245 1362.491(42)	10.0(7)	17.846(1)		0.02
923	19 42 05.91	+40 00 24.0	245 1356.023(3)	1.625(19)	17.952(1)	0.45(7)	0.09
1906[C]	19 41 53.97	+40 01 02.1	245 1355.713(36)	8.1(5)	17.236(1)	0.43(5)	0.03
1934	19 41 53.23	+39 57 32.9	245 1387.555(10)	1.264(12)	18.390(1)	1.1(1)	0.04
2078[B]	19 41 51.31	+39 55 30.5	245 1356.565(5)	1.232(11)	16.7(3)	0.43(5)	0.03
2205[C]	19 41 50.32	+39 58 43.8	245 1383.533(39)	1.824(23)	19.265(2)	1.2(1)	0.06
2529	19 41 46.74	+40 02 14.5	245 1356.461(50)	9.7(6)	17.088(2)	0.42(5)	0.025
3433[H,C]	19 41 50.63	+40 01 52.0	245 1357.43(7)	6.0(3)	19.3(3)		0.03
3731[H,C]	19 41 31.51	+40 01 11.4	245 1358.289(26)	4.56(16)	19.157(2)	0.9(1)	0.04
4327	19 41 24.65	+40 02 37.8	245 1357.763(8)	4.09(49)	16.963(2)	0.6(1)	0.16
4506[C]	19 41 22.63	+40 02 00.2	245 1358.066(25)	10.7(9)	16.818(2)	0.47(6)	0.04
4654[C]	19 41 20.45	+39 56 37.4	245 1355.462(91)	1.39(1)	20.7(4)		0.15
5135[S]	19 41 14.65	+39 54 02.6	245 1357.186(99)	12.5(11)	17.9(3)	0.40(5)	0.02
5853	19 41 06.76	+40 04 57.4	245 1384.985(11)	3.8(1)	18.029(1)	0.51(7)	0.08
5986[C]	19 41 05.17	+40 03 41.3	245 1383.746(31)	8.0(6)	17.474(1)	0.42(5)	0.04
6390[B,C]	19 40 59.82	+39 54 53.4	245 1356.23(6)	4.8(10)	16.6(3)		0.02
6403	19 40 59.99	+39 58 43.8	245 1358.629(81)	3.8(1)	21.384(6)	1.2(1)	0.1
6774[B]	19 40 55.10	+39 57 39.7	245 1387.366(5649)	1.65(2)	18.252(1)	0.44(6)	0.06
6903	19 40 53.52	+40 00 54.3	245 1388.629(74)	6.8(4)	19.175(2)		0.04
7035	19 40 51.76	+39 56 44.2	245 1357.172(55)	10.1(7)	17.1(3)	0.3(1)	0.02
7297[B]	19 40 48.93	+40 04 17.9	245 1354.415(29)	7.4(4)	16.743(2)	0.46(6)	0.04
7569[B]	19 40 45.30	+39 58 40.4	245 1385.955(108)	17.1(25)	17.894(1)	1.0(1)	0.035
7896	19 40 41.55	+40 02 16.7	245 1389.026(10)	2.59(5)	17.295(2)	0.35(5)	0.06
8116[E,C]	19 40 37.96	+39 54 00.7	245 1357.785(32)	2.54(8)	17.0(3)	0.36(5)	0.03
8923	19 40 26.70	+39 55 48.4	245 1356.602(65)	8.2(5)	17.6(3)	0.50(6)	0.015
8931	19 40 26.64	+39 59 32.3	245 1356.615(64)	0.816(5)	18.795(1)		0.03
9410	19 40 20.12	+39 54 46.7	245 1388.426(49)	7.2(5)	19.1(3)	0.56(7)	0.04
9446[E]	19 40 19.92	+40 01 08.3	245 1388.533(83)	1.16(1)	20.730(4)		0.15

Table 8. Details of BY Dra-type systems from CCD 2. The error on the last decimal place is given in brackets. Superscripts indicate the following: [C] close bright companions; [B] blended; [H] in halo of bright star.

Star	RA (J2000.0)	Dec. (J2000.0)	Epoch (HJD)	Period (d)	V (mag)	$V–R$ (mag)	Amp. (mag)
9521[B]	19 40 10.58	+40 16 28.0	245 1358.62(8)	2.39(4)	18.6(4)	0.7(1)	0.07
9555[H]	19 39 23.46	+40 16 19.3	51354.88(4)	4.75(15)	18.3(4)	0.7(1)	0.17
10 146[C]	19 39 52.73	+40 14 56.4	245 1354.55(4)	2.326(42)	19.1(4)		0.06
10 328	19 39 19.93	+40 14 26.7	245 1388.32(3)	3.41(47)	16.9(4)	0.51(7)	0.06
11 544[C]	19 39 23.99	+40 11 34.5	245 1356.51(6)	3.26(8)	20.8(5)	0.7(1)	0.1
12 313	19 40 01.55	+40 09 50.4	245 1384.97(5)	4.7(2)	18.4(4)	0.64(8)	0.02
12 705[B]	19 40 05.63	+40 08 56.7	245 1355.73(8)	9.76(65)	17.2(4)		0.018
12 915	19 39 36.68	+40 08 26.4	245 1357.57(1)	1.39(1)	17.785(3)	0.56(7)	0.13
14 155	19 39 50.03	+40 05 36.1	245 1358.76(7)	7.90(44)	17.025(1)	0.38(5)	0.015
14 159	19 39 49.67	+40 05 35.9	245 1384.02(4)	6.85(34)	19.058(1)	1.1(1)	0.12
14 163[C]	19 39 27.86	+40 05 35.4	245 1358.56(10)	2.73(5)	16.548(2)		0.027
14 597[H]	19 39 32.37	+40 04 30.5	245 1358.48(8)	2.1(2)	16.745(2)	0.72(9)	0.025
14 636	19 39 21.49	+40 04 26.1	245 1354.5(2)	7.56(313)	16.9(4)	0.38(5)	>0.012
14 760[B]	19 40 08.25	+40 04 08.3	245 1357.579(4)	0.3896(3)	17.1(4)	0.39(5)	0.07
15 251	19 40 01.22	+40 02 57.3	245 1360.57(1)	0.327(4)	20.212(3)		0.13
15 607	19 39 32.55	+40 02 04.9	245 1354.48(7)	1.29(6)	18.884(1)	0.72(9)	0.055
16 159	19 39 39.81	+40 00 45.5	245 1355.60(3)	0.67(2)	18.157(1)	0.47(6)	>0.03
17 127[C]	19 39 25.15	+39 58 25.6	245 1354.34(7)	2.93(6)	19.2(4)	1.2(1)	0.035
18 314[H]	19 40 05.82	+39 55 33.4	245 1355.01(6)	2.81(6)	17.7(4)	0.32(9)	0.018

Table 9. Details of BY Dra-type systems from CCD 3. The error on the last decimal place is given in brackets. Superscripts indicate the following: [C] close bright companions; [B] blended; [F] close to flaw in image, e.g. dead column, light leak or diffraction spike; [H] in halo of bright star.

Star	RA (J2000.0)	Dec. (J2000.0)	Epoch (HJD)	Period (d)	V (mag)	V–R (mag)	Amp. (mag)
20 127	19 42 06.92	+40 20 25.6	245 1389.54(8)	7.6(4)	17.315(1)	0.3(1)	0.015
20 184	19 42 06.33	+40 24 53.9	245 1385.16(2)	3.046(7)	20.060(2)		0.04
21 326	19 41 51.92	+40 20 31.1	245 1385.46(6)	3.83(10)	18.610(1)		0.03
21 465	19 41 50.22	+40 20 26.5	245 1387.94(6)	4.18(17)	17.858(1)		0.03
21 962	19 41 43.72	+40 17 23.1	245 1387.60(2)	0.599(2)	18.394(1)	0.48(6)	0.025
22 389[C]	19 41 38.84	+40 21 53.1	245 1387.33(3)	5.5(2)	19.934(2)		0.1
23 064	19 41 30.20	+40 22 17.6	245 1355.04(8)	6.3(3)	17.252(1)		0.02
23 455[H]	19 41 26.52	+40 27 32.7	245 1387.34(3)	4.1(2)	18.6(4)		0.07
24 157	19 41 16.50	+40 18 17.2	245 1385.18(6)	6.7(3)	20.047(2)		0.04
24 808[C]	19 41 08.34	+40 21 20.9	245 1356.10(4)	12.1(102)	18.654(1)	0.51(7)	0.028
25 731[C]	19 40 57.05	+40 19 14.8	245 1383.87(4)	2.30(4)	21.011(5)	0.9(1)	0.1
25 940	19 40 55.25	+40 27 13.5	245 1384.593(9)	4.45(13)	17.7(3)	0.60(8)	0.08
26 763[F]	19 40 43.57	+40 17 26.5	245 1385.24(3)	3.18(7)	19.3(4)	0.8(1)	0.08
26 924[B]	19 40 42.10	+40 22 21.5	245 1356.0(1)	13.3(8)	17.5(3)	0.9(1)	0.015
27 061[C,F]	19 40 40.73	+40 26 22.6	245 1384.05(4)	3.00(7)	17.9(3)		0.012
27 149	19 40 39.79	+40 27 47.7	245 1354.8(2)	19.82(26)	18.0(3)	0.52(6)	>0.02
27 192	19 40 38.63	+40 22 15.8	245 1353.9(2)	14.6(15)	18.358(1)		0.015
27 202	19 40 38.61	+40 23 02.6	245 1358.6(2)	19.3(26)	17.974(1)		0.017
27 704	19 40 32.03	+40 26 04.0	245 1386.96(60)	6.7(3)	17.4(3)	0.56(7)	0.03
28 204[C]	19 40 25.16	+40 23 17.0	245 1389.54(1)	1.095(9)	18.208(1)	0.9(1)	0.06

tens of days, with amplitudes between 0.05–0.5 mag. Alekseev (2000) found that the majority (80 per cent) of BY Dra stars do not exceed an amplitude of 0.15 mag, and our data conform to this finding.

A number of these stars show changes in the morphology and amplitude of the light-curve variations from one half of the data set to the next. The light curves of stars 923, 4327 and 7896 clearly show this effect. As the second half of the data set was taken after a one-month interval, these variations are attributed to changing spot coverage on the surface of the stars. In some cases, the period apparent from the sinusoidal variations changes noticeably from one month to the next. This variation in the period would be expected from star-spots appearing at different latitudes on the stellar surface, and is a hallmark of differential rotation on the star. In a few cases, the light curves of affected stars have not been folded on the period for the sake of clarity.

Stars 14 155 and 14 159 form a visual binary. The stars are close, but distinct and separated on the reference frame. We note these stars both show variations occurring at differing phases, so it is likely that both stars are separately variable.

Table 11 gives a list of stars which vary either irregularly or on time-scales similar to or longer than that of the data set. Some of these may be active stars, but our data set is insufficient to determine their ephemerides. In some cases, the variation is only slightly greater than the uncertainty, and all the stars in this section need further observations to confirm their nature. These light curves are given in Fig. 10. We present the period and amplitude distributions for this class of variable in Fig. 11.

Fig. 12 plots *V–R* colour against period for all BY Dra stars for which these have been determined. There are some instances of widely scattered points in this diagram, often in cases where the period cannot be accurately determined from the data. However, the distribution shows a general trend towards shorter periods for redder stars. This is expected, as G stars (*V–R* ∼ 0.54) spin down rapidly. We find examples of early-type stars with periods under 5 d, which

would imply that these stars belong to a young population. However, our sample necessarily consists of a mix of field and cluster stars covering a range of ages, and membership information is required to distinguish the two.

Fig. 12 shows a few examples of stars with anomalously high rotation periods for their colour. It is always possible that these stars are composites or binaries, which would alter their apparent colour. However, it is common for the size and latitude of active regions of BY Dras to vary or even disappear, making accurate period determination difficult.

Superimposed on Fig. 12 for comparison are the periods determined for the activity cycles shown by the RS CVn stars in the sample. The colours of these stars are known to be blends of the binary, therefore offsetting these points horizontally, but it is interesting to note that they follow roughly the same distribution as the BY Dras. Close binaries can cause spin-up of their components.

4.4 Variable stars of other types

Table 12 lists five stars whose more unusual variability does not fall into any of the above classes (in addition to the four found in CCD 4). The first of these stars, 2203, appears to be a Cepheid. A *V–R* colour of 0.6 is consistent with a pulsating giant star of spectral type F–K, class Ib–II, as is the period of ∼5 d.

The second half of the light curve of star 27 232 shows a Cepheid-like profile; unfortunately, noise obscures the first half of the data set and we are unable to confirm this classification. Its *V–R* colour of 0.7 could indicate a late G-type giant, while its amplitude of 0.1 mag would be reasonable. However, until further work is done, this remains a suggestion only.

We believe star 4218 to be another type of pulsating star, this time an RR Lyrae. No *V–R* colour was available for this star, but Kalirai et al. (2001) derived a *B–V* of 0.253 ± 0.002, which is consistent with it being a ∼A III class. The amplitude is within the accepted
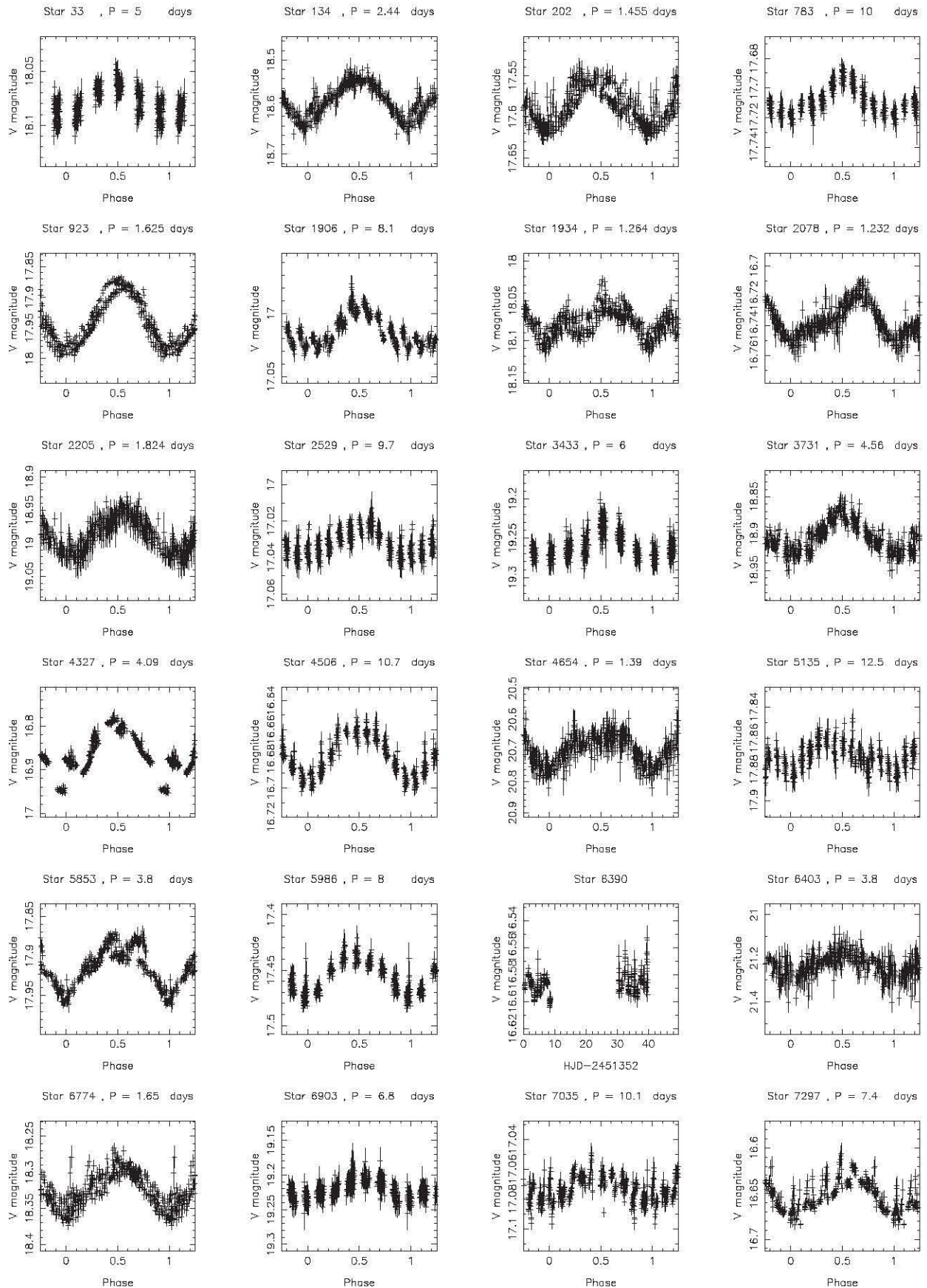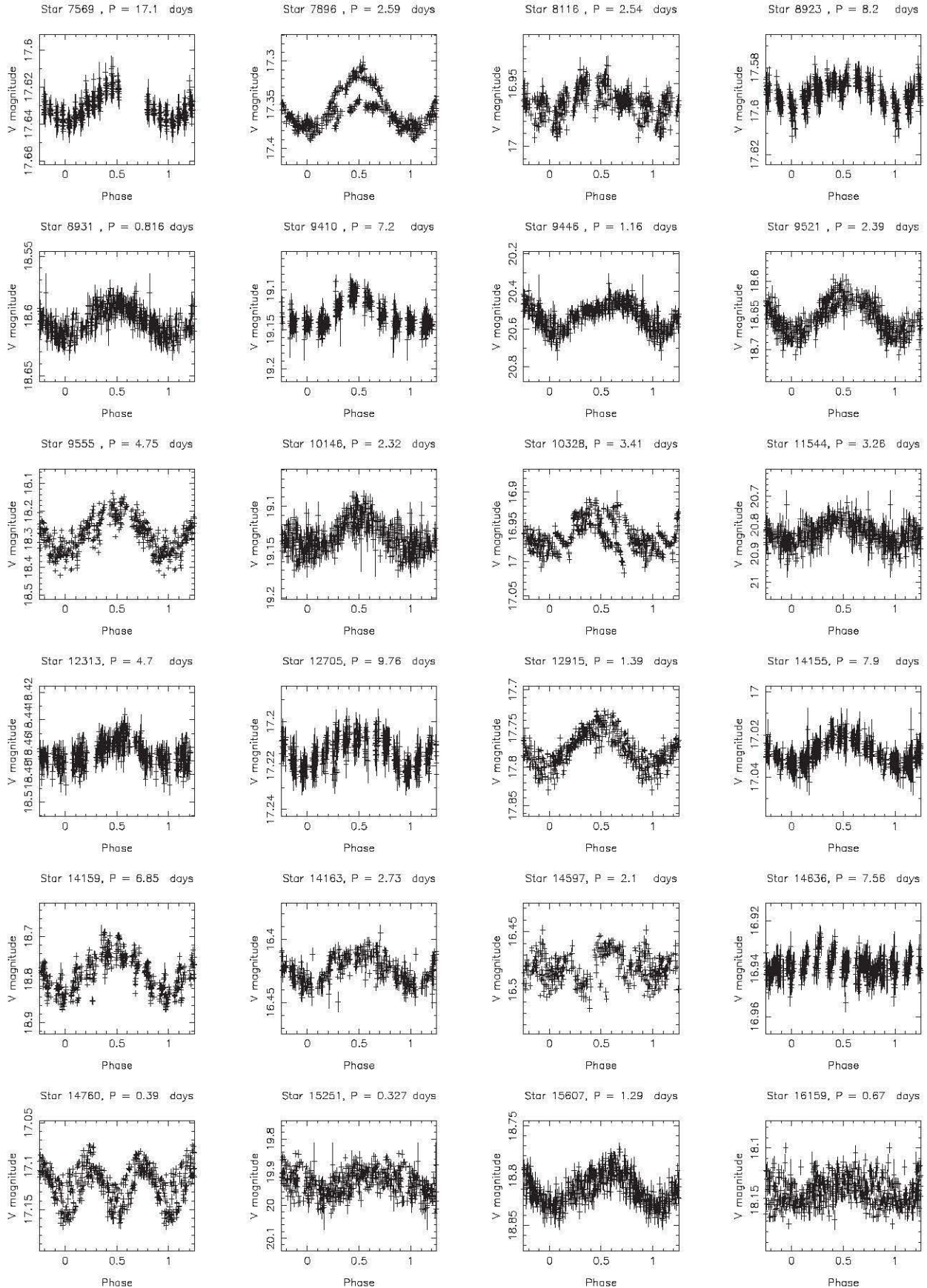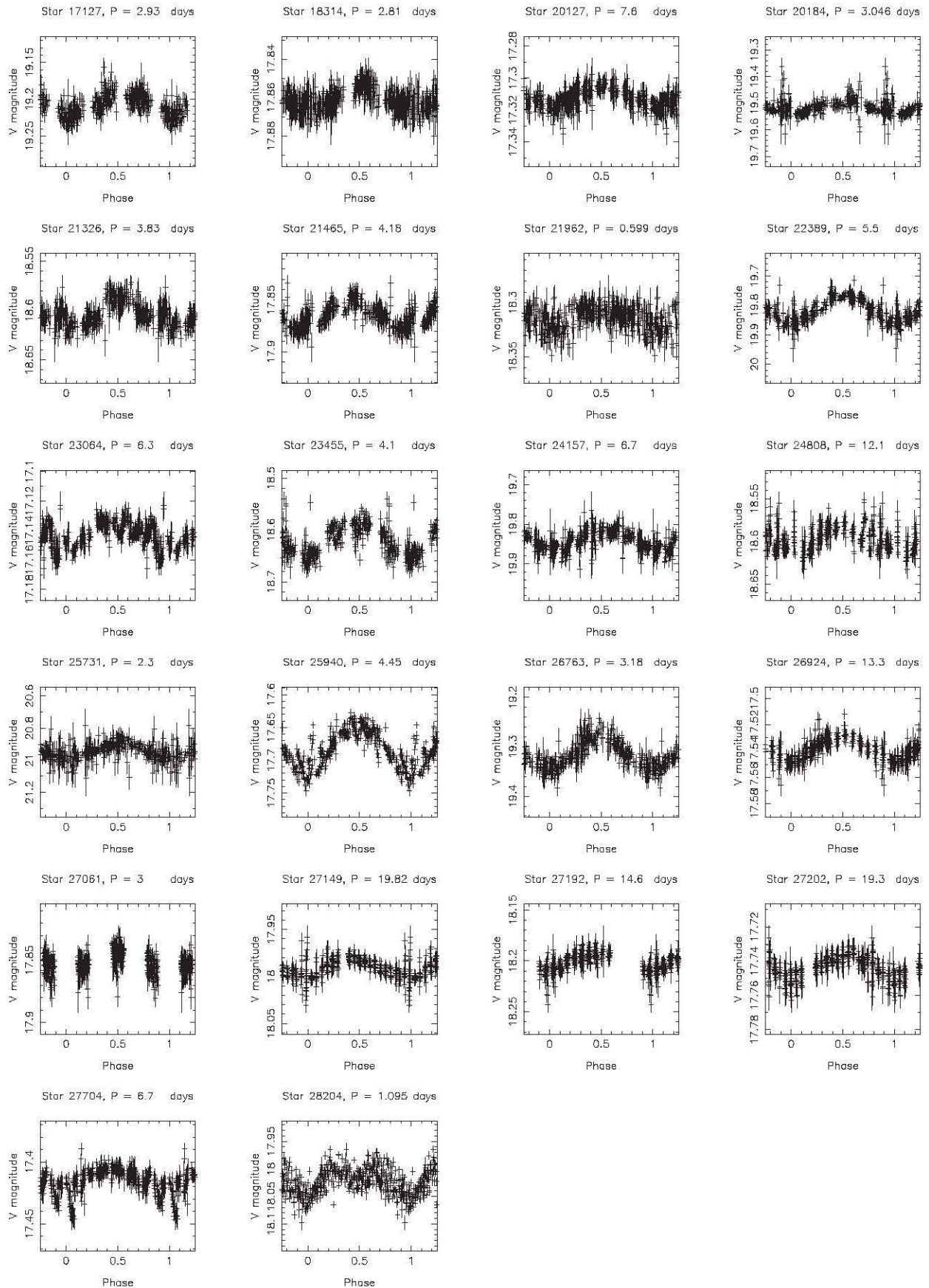
Figure 7. Light curves of the BY Dra systems.

Figure 8. Light curves of the BY Dra systems.

Figure 9. Light curves of the BY Dra systems.

Table 10. Details of BY Dra-type systems from CCD 4. The error on the last decimal place is given in brackets. Superscript [C] indicates close bright companion. Column 1 lists the star's original ID numbers in brackets.

Star	RA (J2000.0)	Dec. (J2000.0)	Epoch (HJD)	Period (d)	V (mag)	V–R (mag)	Amp. (mag)
30 392 (1815)	19 41 51.38	+40 12 33.6	245 1388.61(1)	0.733(4)	19.400(2)	0.9(1)	0.06
30 970 (2393)	19 41 44.46	+40 14 23.8	245 1356.56(4)	1.9(2)	18.765(1)	0.54(7)	0.04
31 153 (2576)	19 41 41.61	+40 07 03.1	245 1389.6(3)	1.37(1)	18.833(1)	1.2(2)	0.14
31 703 (3126)[C]	19 41 36.05	+40 16 19.9	245 1384.62(6)	5.4(2)	19.939(2)		0.05
31 704 (3127)	19 41 35.88	+40 13 53.3	245 1386.19(2)	3.5(1)	19.758(2)	0.8(1)	0.08
32 580 (4003)	19 41 26.77	+40 10 49.5	245 1384.49(2)	3.9(1)	18.2(4)	0.64(9)	0.08
33 061 (4484)	19 41 22.18	+40 10 11.4	245 1357.31(4)	6.3(3)	19.1(4)	0.49(7)	0.09
34 438 (5861)	19 41 09.75	+40 10 38.1	245 1387.11(5)	6.5(3)	19.120(2)		0.06
36 288 (7711)	19 40 48.43	+40 16 19.3	245 1357.39(3)	4.2(1)	20.677(4)	0.5(2)	0.39

Table 11. Details of long-period variable systems. The error on the last decimal place is given in brackets. Superscripts indicate the following: [C] close bright companions; [E] close to edge of frame; [S] suspected variable.

Star	RA (J2000.0)	Dec. (J2000.0)	V (mag)	V–R (mag)	Amp. (mag)
5595	19 41 09.65	+40 00 02.5	18.004(1)		>0.03
5669	19 41 08.88	+39 59 43.9	18.191(1)	0.46(6)	0.03
6140[S]	19 41 03.46	+40 03 17.2	18.121(1)	0.42(5)	>0.015
6464[S]	19 40 59.57	+40 04 15.9	18.044(1)		>0.02
12 415	19 39 53.70	+40 09 35.4	18.2(4)		>0.03
14 602	19 40 05.26	+40 04 29.4	19.1(4)		0.03
15 801[C]	19 39 48.84	+40 01 34.9	16.447(2)	0.43(5)	>0.015
17 737	19 39 22.66	+39 57 01.2	17.2(4)	0.37(5)	>0.025
21 418	19 41 50.96	+40 24 22.5	17.273(1)		0.02
21 807	19 41 46.25	+40 27 33.9	17.8(3)	0.46(6)	>0.04
22 991[E]	19 41 31.40	+40 28 11.3	17.5(3)	0.3(1)	0.02
25 150[C]	19 41 03.88	+40 21 09.8	18.556(1)		0.02
26 162	19 40 51.61	+40 18 20.0	20.166(3)		0.03

range, and the period lies only slightly outside the generally accepted range

The classification of stars 8824 and 12 486 remains elusive, but they may be of the δ Scuti type. Determining the ephemeris of 8824 has proven difficult, and it is likely that this star exhibits multiple periods. Fig. 13 shows its periodogram, and the light curve in Fig. 14 has not been phased. Star 12 486 on the other hand does show a clear dominant periodicity.

In Street et al. (2002) a number of stars were identified whose variability was suspected but not confirmed. We include their data in Table 13.
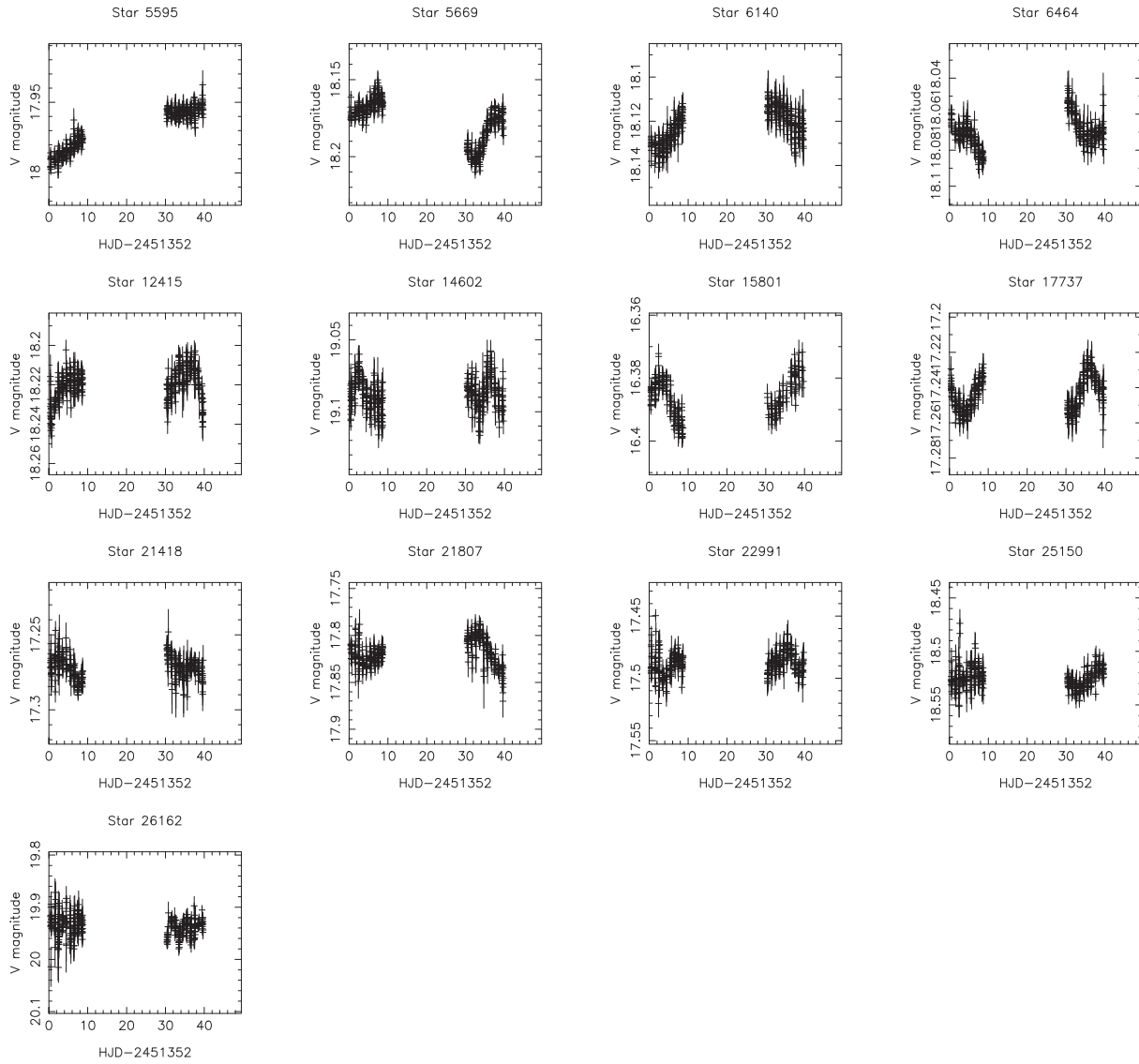
5 CONCLUSIONS

We present long-baseline Sloan r' photometry for $\sim$28 500 stars in the field of the intermediate-age open cluster NGC 6819 covered by CCDs 1–3 of the INT/WFC. We have identified 141 variable stars in this sample, bringing the total number of variables found in this field to 178. With some of these stars we have stated reasons for caution, owing chiefly to blending, low amplitude, high background and proximity to the edge of the frame. This sample breaks down into common types of variability as follows: 53 eclipsing binaries and 70 BY Dra-type activity. A further 13 stars exhibit variability on time-scales longer than the data set. The nature of these latter will remain inconclusive until more data are available. Finally, five stars

were found to show more unusual types of variability; these include a Cepheid, an RR Lyrae and two suspected δ Scutis. However, we urge caution regarding these classifications until confirmation is possible via spectroscopy and/or further photometric observations.
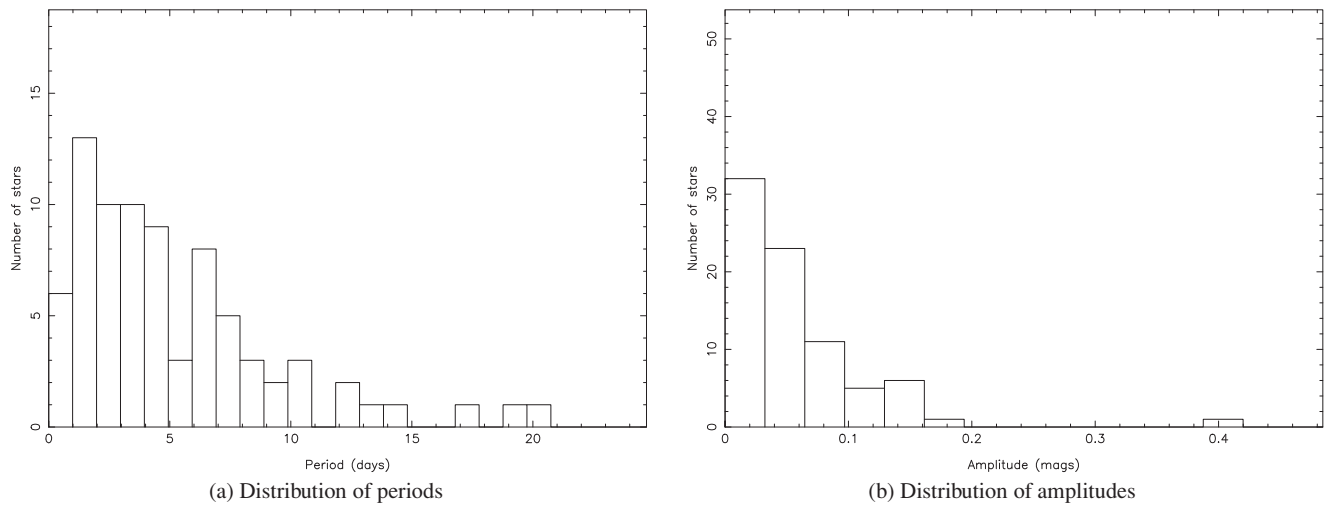
Our survey results contribute to a growing body of observations produced by a variety of variable star surveys. Groot et al. (2003), for example, describe a project using the same INT/WFC equipment. Their survey bears many similarities to our work in terms of magnitude range (17–24 mag), photometric precision achieved (down to 5 mmag) and the high cadence, intensive observation strategy. However, Groot et al. (2003) are targeting mid- and high-Galactic latitude non-cluster fields, and consequently anticipate the discovery of a population of variables including CVs, RR Lyraes, optical transients and Solar system objects. A number of projects focus specifically on open clusters (e.g. Kaluzny, Krzemiński & Mazur 1996; Mochejska & Kaluzny 1999; Mochejska, Stanek & Kaluzny 2003; Paunzen et al. 2004). These observations often provide the first time-series data available on cluster in this magnitude range (and hence spectral type). The studies of cluster populations, with their common age, metallicity, history, etc., play a crucial role in testing models of stellar evolution. Our work provides the first such deep survey of NGC 6819. Because the cluster radius is small relative to the WFC field of view, our survey also provides a direct comparison sample of variables from the field at the same galactic latitude. One natural progression of this work would be a study of the stellar proper motions to unambiguously establish cluster membership, and spectroscopy to determine the variables' spectral type and confirm their classifications. In particular, we recommend further investigation of the short-period EA binaries, a number of which (e.g. 13 770 and 22 431) have colours indicating late-type stars. Such binaries are central to constraining the mass–radius relation for low-mass stars.

Star 5595

Star 5669

Star 6140

Star 6464

Star 12415

Star 14602

Star 15801

Star 17737

Star 21418

Star 21807

Star 22991

Star 25150

Star 26162

Figure 10. Light curves of the long-period variable systems.

(a) Distribution of periods

(b) Distribution of amplitudes

**Figure 11.** Distributions of the BY Dra population according to period and amplitude.

Table 12. Details of variable stars of other types. The error on the last decimal place is given in brackets. Superscripts indicate the following: [C] close bright companions; [H] in halo of bright star; [F] close to flaw in image, e.g. dead column, light leak or diffraction spike. Column 1 lists the star's original ID numbers in brackets.

| Star	RA (J2000.0)	Dec. (J2000.0)	Epoch (HJD)	Period (d)	V (mag)	V–R (mag)	Amp. (mag)	Type
2203[C]	19 41 50.63	+40 01 52.0	245 1357.257(11)	4.94(16)	17.208(1)	0.6(1)	0.25	Cepheid
4218[H]	19 41 25.89	+40 03 07.7	245 1385.593(3)	1.80(2)	19.280(2)		0.13	RR Lyr
8824	19 40 27.99	+39 54 41.4	multi	periodic?	17.0(3)	0.2(1)	0.38	δ Scuti
12 486[H]	19 39 37.08	+40 09 24.7	245 1354.472(157)	0.04291(1)	16.937(2)	0.18(6)	0.04	δ Scuti
27 232	19 40 38.02	+40 21 29.2	245 1382.19(5)	8.0(4)	20.914(4)	0.7(1)	0.1	Cepheid?
28 801 (224)	19 42 11.66	+40 06 48.7	245 1384.323(5)	11.5(20)	17.611(1)		0.02	Unclass
31 182 (2605)[F]	19 41 41.69	+40 11 41.5	245 1389.64(5)	9.6(6)	18.474(1)	0.65(8)	0.04	Unclass
36 709 (8132)	19 40 41.60	+40 07 46.9	–	–	19.2(5)	0.4(2)	0.45	Cepheid?
37 407 (8830)	19 40 32.00	+40 10 40.3	245 1384.61(1)	10.9(8)	18.402(1)		0.15	Unclass
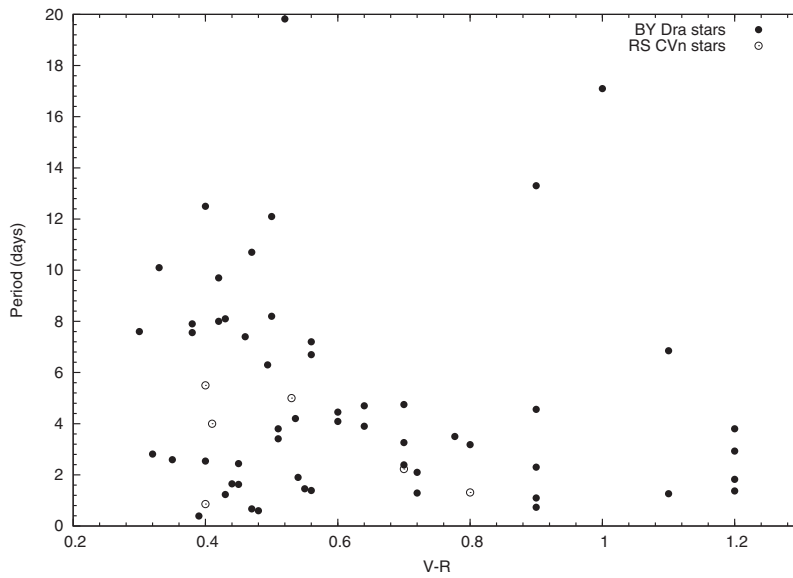
Figure 12. Distribution of BY Dra periods with *V–R* colour, superimposed with the same data derived from the activity shown by the RS CVn stars for comparison.
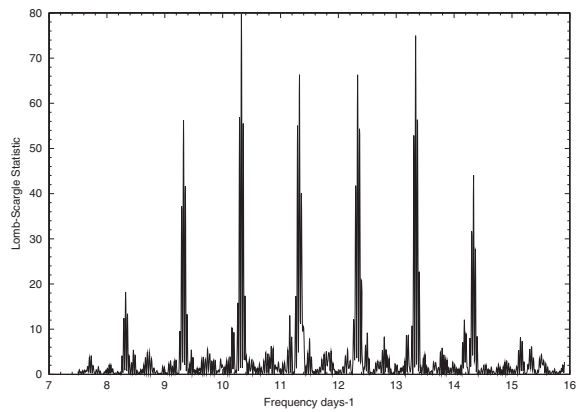
Figure 13. Periodogram of the data for star 8824, a suspected δ Scuti, showing multiple strong peaks in frequency.

Table 13. Details of suspected variable stars. The error on the last decimal place is given in brackets. Column 1 lists the star's original ID number in brackets. Following reanalysis, star 30 608 (2031) is now below the threshold for variability.

Star	RA (J2000.0)	Dec. (J2000.0)	V (mag)	V–R (mag)	Amp. (mag)
30 608 (2031)	19 41 48.92	+40 14 12.3	18.334(1)		0.02
31 078 (2501)	19 41 42.74	+40 08 40.2	19.427(2)	0.59(8)	0.06
31 402 (2825)	19 41 39.15	+40 13 26.8	19.693(2)	0.8(2)	0.07 (act)
					0.25 (ecl)
31 813 (3236)	19 41 34.26	+40 06 34.9	17.027(1)		0.05
32 455 (3878)	19 41 28.16	+40 12 32.9	17.269(1)	0.46(6)	0.025
32 916 (4339)	19 41 23.67	+40 11 52.2	17.0(4)		0.018
33 948 (5371)	19 41 14.72	+40 12 14.2	18.247(1)	0.57(7)	0.042
34 167 (5590)	19 41 12.60	+40 12 06.5	18.7(4)		0.07
36 729 (8152)	19 40 41.72	+40 13 37.7	19.499(2)	0.53(7)	0.06
37 318 (8741)	19 40 33.50	+40 15 57.6	18.520(1)	1.1(1)	0.07
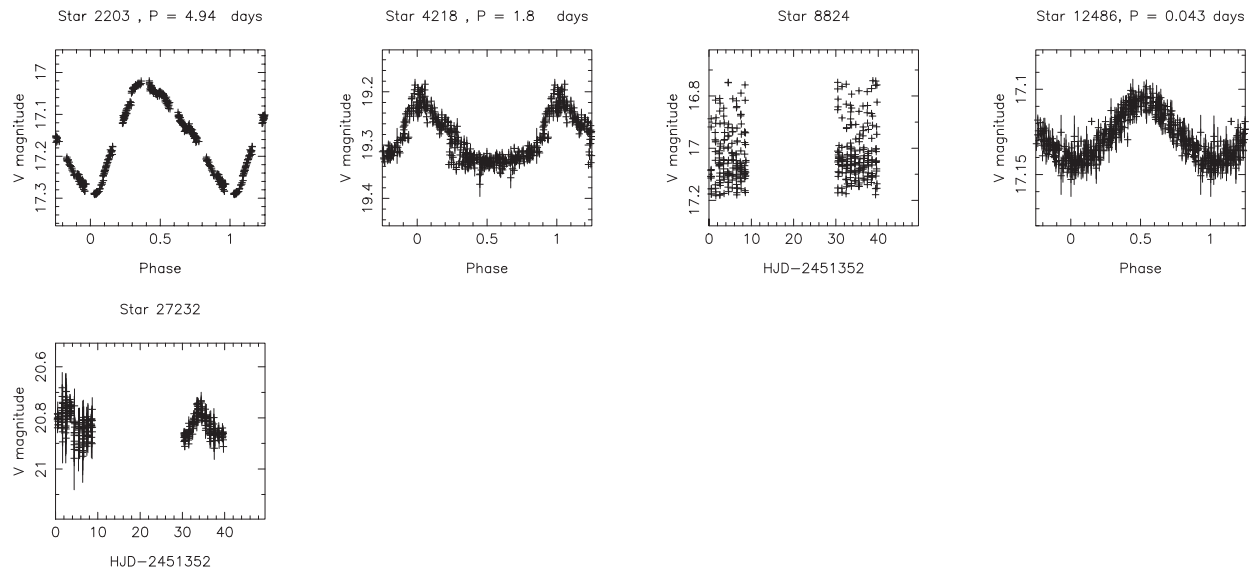
Figure 14. Phased light curves of stars showing other types of variability.

REFERENCES

Alekseev I. Y., 2000, SvA, 77, 784
Groot P. et al., 2003, MNRAS, 339, 427
Kalirai J. S. et al., 2001, AJ, 122, 266
Kaluzny J., Krzemiński W., Mazur B., 1996, A&AS, 118, 303
Mochejska B. J., Kaluzny J., 1999, Acta Astron., 49, 351
Mochejska B. J., Stanek K. Z., Kaluzny J., 2003, ApJ, 125, 3175
Paunzen E., Zwintz K., Maitzen H. M., Pintado O. I., Rode-Paunzen M., 2004, A&A, 418, 99
Press W., Flannery B., Teukolsky S., Vetterling W., 1992, Numerical Recipes in Fortran 77, Vol. 1. Cambridge Univ. Press, Cambridge
Rucinski S. M., Duerbeck H. W., 1997, PASP, 109, 1340
Stetson P. B., 1987, PASP, 99, 191
Street R. A. et al., 2002, MNRAS, 330, 737 (Paper I)
Street R. A. et al., 2003, MNRAS, 340, 1287

This paper has been typeset from a TEX/LATEX file prepared by the author.